ANALYSIS ANS LWR PHYSICS BENCHMARK PROBLEMS BY SH AND SPS METHODS

Laletin N.I., Sultanov N.V., Kovalishin A.A.
RRC "Kurchatov institute"
Kurchatov sq. 1
123182 Moscow, Russia
laletin@adis.vver.kiae.ru; nsult@adis.vver.kiae.ru; kaa@adis.vver.kiae.ru

Keywords: reactor, neutron, calculation, method

ABSTRACT

Results of SHM calculations applied to PWR reactors are presented to demonstrate here the potential of the Surface Harmonics Method (SHM) and the Surface Pseudo-Sources Method (SPSM). These methods indeed were developed as a solution to the problem of improvement of neutron field calculations in the cores of nuclear reactors with non uniform lattices.

1. INTRODUCTION

The following quotation from (Taiwo,1998) seems to be good to start the paper with:

"The PWR Lattice Benchmark Problems were defined by the ANS Committee on Reactor Physics Benchmarks in mid-1996, as a means of intercomparing and validating various calculation methodologies and codes used for analyzing light water reactor (LWR) cores". Besides the above-mentioned general purpose common for a number of researches, we should also define the aims of the current paper. It is quite essential to demonstrate here the potential of the Surface Harmonics Method (SHM) and the Surface Pseudo-Sources Method (SPSM). These methods indeed were developed as a solution to the problem of improvement of neutron field calculations in the active zones of nuclear reactors with various violations in non uniform lattice. Actually the group of tests under consideration in this paper is not the best one for demonstrating our methods. First of all these experimental cores are not representative enough as they are not sufficient non uniform lattices. In this sense, experimental cores, that had been studied by Temporal International Collective (TIC) for Joint Research into the Physics of WWER-type Reactors in Budapest for a number of years, seem to be more interesting for comparison of different engineer methodologies. We would suggest TIC cores as a research subject, similar to PWR already used, to the ANS Ad Hoc Committee on Reactor Physics Benchmarks. However since a large number of researchers have already carried out their calculations of PWR cores, it is surely interesting to compare those results with ours as well.

It should also been noted that most of calculations that had been fulfilled (see the corresponding survey in (Parish, 1998)) were benchmark ones, i.e. either Monte-Carlo methods or S_n-methods with detailed enough dissection in space and corners were applied in the codes used. Such computations are mostly aimed at estimating the quality of micro-constant libraries used. The only exceptions are calculation results

provided by Gemesh (Mohanakristan, 1998) diffusion code and DIF-3-NODAL (Taiwo, 1998) code. It seems also unclear what option of LWR-WIMS code has been used in this calculation series (Parish, 1998) - diffusion SAN or transport option CACTUS. We would consider all those results in more details lately in the paper when analyzing results of our computations. For the time being we would like to emphasize that our methods allow one to obtain results of the same precision as those provided by benchmark calculations and, at the same time, preserve high speed of computation common for "engineer" codes.

2. THE PWR LATTICE BENCHMARK PROBLEMS

2.1. Description of experiments and benchmark problems formulation

Description of experiments carried out combined with formulation of benchmark problems is presented in initial paper of the ANS Committee and in all papers devoted to computation of those problems. Nevertheless for convenience of a reader we will repeat that data here by merely citing some parts of initial document of the ANS Committee (Diamond, 1996).

"The experiments were performed inside a large aluminium tank containing borated water, UO_2 fuel pins, and a number of so-called perturbing pins. The fuel pins contained low-enriched uranium (LEU) and were clad in aluminum. The water contained soluble boron in the form of dissolved boric acid (H_3BO_3). The water height was exactly 145 cm, and the boron concentration in the water was adjusted until each experimental configuration was slightly supercritical, with a value of 1.0007 for $K_{eff.}$ The soluble boron concentration for each experiment was determined by titration and reported in units of parts per million by weight (ppm) in water. The standard deviation for each soluble boron concentration is ±3ppm

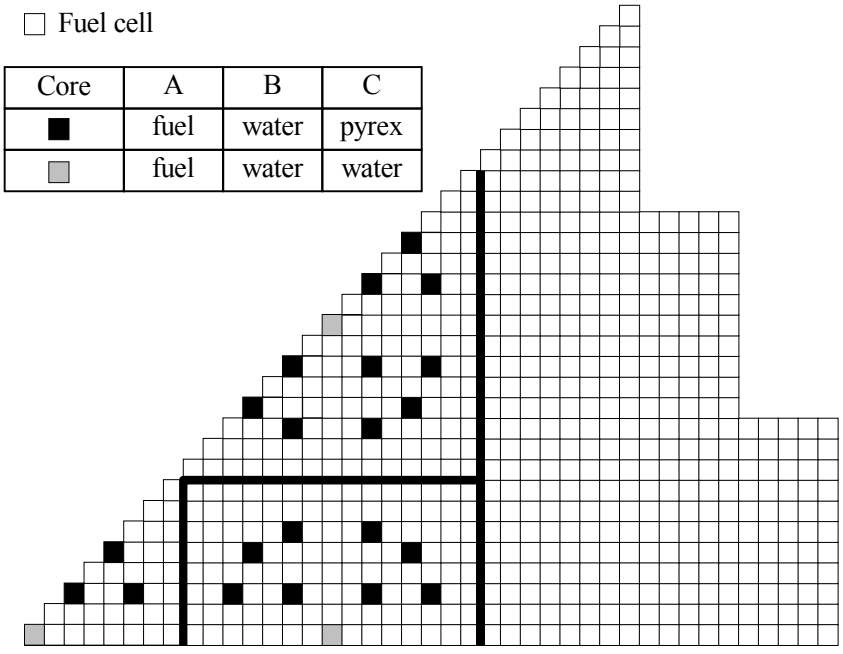

Fig.1 PWR core, 1/8 part

For most of these experiments, the central region of the core closely resembled a 3×3 array of pressurized water reactor (PWR) fuel assemblies with fuel pins arranged in a 15×15 lattice. The nine assemblies were surrounded by a driver region of LEU fuel pins identical to those in the assemblies. The driver region had an irregular boundary. The region between the driver boundary and the inner wall of the tank contained only water.

The assemblies consist of a 15×15 array of fuel pins, water holes, and perturbing pins. All of the loadings are laid out on a square pitch of 1.63576 cm. Assembly type A contains fuel rods in all locations and, therefore, is indistinguishable from the driver region. Assembly type B contains 17 water holes arranged in the same configuration as a standard 15×15 fuel assembly for a commercial PWR. Assembly type C is identical to type B except that pyrex rods have been inserted into all of the water holes except the central hole."

2.2. Methodology of calculations

Computations have been carried out using WIMS-SH and SHM-QUADRO codes. Solutions of the finite-difference equations of the following form are basic for all calculations:

$$\frac{2}{a^2}\sum_{j=1}^{4}\mathbf{\Lambda_{jk}}\left(\vec{\Phi}_j-\vec{\Phi}_k\right)-\mathbf{\Sigma}_k\vec{\Phi}_k+\frac{1}{K_{eff}}\mathbf{\nu_f\Sigma_f}\vec{\Phi}_k=0 \qquad (1)$$

The meaning and ways of calculating required coefficients will be different for three series of calculations described below.

1. Let us define computations of the first series as "traditional" since similar scheme of calculation is nowadays applied in many codes for computing both inner-assembly distributions and active zones. For these calculations variables in equation (1) are defined as:

$\vec{\Phi}_k$ is a vector consists of average group fluxes in K-th cell;

Σ- is a matrix with elements that are cross-section absorptions and inter-group transitions averaged in a cell;

$\mathbf{F_f}$- is a matrix of neutron multiplication in groups;

$K_{eff.}$- is a multiplication factor;

$\mathbf{\Delta_{jk}}$ is a diagonal matrix with elements of the form: $\mathbf{\Delta_{ik}^{gg}}=\dfrac{D_i^g D_k^g}{D_i^g+D_k^g}$, $\qquad D_i^g=\dfrac{1}{3\langle\Sigma_{tr}\rangle}$

All group cross-sections were calculated by RACIYA option of WIMS-SH complex, which is based on SPSM. A 28-group energy dissection with boundaries presented in Table 1 has been used during the computation. The dissection is similar to that of mini-WIMS recommended in the report on LWR-WIMS.

Table1. Boundaries of energy groups under different dissections of energy axis.

Groups				Higher boundary (eV)
4	8	15	28	
1	1	1	1	$10.0X10^6$
	2	2	2	$1.353X10^6$
2	3	3	3	$821X10^3$
			4	67340
3	4	4	5	9118
			6	148.728
		5	7	15.968
			8	9.877
	5	6	9	4.0
			10	3.30
		7	11	2.60
			12	2.10
		8	13	1.30
			14	1.15
		9	15	1.097
			16	1.020
		10	17	0.972
			18	0.950
			19	0.850
4	6	11	20	0.625
			21	0.400
		12	22	0.320
	7		23	0.250
		13	24	0.140
			25	0.067
	8	14	26	0.050
		15	27	0.030
			28	0.015

The following problems are solved here:

(i) For a cell with fuel the problem with zero-current boundary condition was solved, i.e. the problem of determining K_∞. All necessary cross-sections were averaged on space-energy neutron distribution obtained and prepared for further

calculations of 4, 8, and 15 group constants. This set of groups has been used for other series of calculations as well.

(ii) For cells with absorber and water enlarged cells were created with eight cells with fuel surrounding the central cell under consideration. Again zero-current boundary conditions for enlarged cells were applied. All necessary cross-sections for investigated central cells were averaged on space-energy distribution obtained and prepared for further calculations of 4, 8, and 15 group constants.

The leakage on Z was accounted in a standard manner by adding DB_z^2 term to absorption cross-section.

Micro cross-sections in this calculation were taken from WIMS-D4 library. Note that the nuclide 2238.4 was recommended by authors of WIMS-D4 code, It was applied for U-238. It is a common knowledge that the cross-section of resonance absorption of neutrons in this nuclide is artificially undervalued comparing with initial values obtained from UKNDL files. As a result, obtained multiplication factors become agreeable with those provided by experiments. Our calculations of various cores TRX, BAPL, and others also support this fact. Additional computations with other constants for U-238 and U-235 (Laletin, 1983) have also been carried out. We will point out the aim and some conclusions derived out of those calculations below when discussing obtained results.

We were using two libraries of cross-sections when calculating the benchmark. The first one is the general library of WIMS-D4 and the second one included cross-sections of U-235 and U-238, which have been corrected. Both libraries do not agree with libraries applied in publications from the reference list of [Parish,1998]. It does not take place even for papers, which are dedicated to the benchmark with WIMS applied. But the libraries used there have been either totally different from our general libraries or modified partially. Two modifications of cross-sections of U-235 and U-238 have made our library closer to the libraries of papers [Glushkov, 1995]. However there are still some differences in the rest nuclides.

The water reflector was calculated using the same set of constants as for the cells with water inside the zone. A series of calculations of core with various external reflector boundaries (with zero-current flux) gave us a boundary, further enlargement of which failed to change the result.

2. Let us call the second series of calculations an “SHM-homogenous”. In these calculations the same equation (1) is used but with coefficients determined in other way. Suppose that cells are homogenous with average 4, 8, 15 group cross-sections. Let us apply <3F> approximation for the SHM method (Laletin, 1999) for deriving equation (1) and corresponding coefficients.

Symmetric and antisymmetric trial functions for cells and corresponding matrixes $\mathbf{S_0}$, $\mathbf{S_1}$ were obtained using ANDIF code. The algorithm realized in this code is based on analytically inverted multi-group diffusion equation for problems with corresponding boundary conditions. Note that matrixes $\mathbf{S_0}$, $\mathbf{S_1}$ can be presented in the form: $\mathbf{S_0=\Phi_s\,(E_s)^{-1}}$ и $\mathbf{S_1=\Phi_{as}\,(E_{as})^{-1}}$. Here matrixes $\mathbf{\Phi_s}$ and $\mathbf{E_s}$ have the form:

$$\mathbf{E_s} = \begin{pmatrix} 1 & 0 & \cdots & 0 \\ 0 & 1 & \cdots & 0 \\ \vdots & \vdots & \ddots & \vdots \\ 0 & 0 & \cdots & 1 \end{pmatrix} \text{ and } \mathbf{\Phi_s} = \begin{pmatrix} f_s^{11} & f_s^{12} & \cdots & f_s^{1G} \\ f_s^{21} & f_s^{22} & \cdots & f_s^{2G} \\ \vdots & \vdots & \ddots & \vdots \\ f_s^{G1} & f_s^{G2} & \cdots & f_s^{GG} \end{pmatrix}$$

Figure 2 shows the dependence of $\mathbf{E_s}(r_s)$ and $\mathbf{E_{as}}(r_s)$ on cell boundary coordinates.

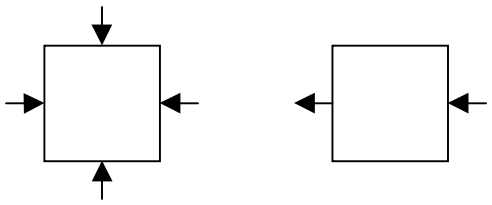

Figure 2. Dependence of currents on cell boundaries.

Values $f_s^{gg'}$ are neutron fluxes averaged on boundary for the group g in the problem with incoming net current in the group g'.

Matrix $\mathbf{S_1}=\mathbf{\Phi_{as}}\,(\mathbf{E_{as}})^{-1}$ has the same structure as $\mathbf{S_0}$ with the only exception that dependence of incoming current is different here (see Figure 2.). Values $f_{as}^{gg'}$ here are neutron fluxes for the group g averaged on right side in the problem with incoming net current in the group g'.

Coefficients in equation (1) are obtained from matrixes $\mathbf{S_0}$ and $\mathbf{S_1}$ using the following formulas:

$$\begin{aligned} &\vec{\Phi}_k = \left(\mathbf{S_{0,k}} - \mathbf{S_{1,k}}\right)\vec{I}_s \\ &\mathbf{D_k} = \frac{a}{2}\mathbf{S_{1,k}^{-1}}; \quad \Delta_{i,k} = \mathbf{D}_i\left(\mathbf{D}_i + \mathbf{D_k}\right)^{-1}\mathbf{D_k}; \\ &\mathbf{ó}_k = \mathbf{ó_{af,k}}\mathbf{ä}_k; \qquad \mathbf{ó_{af,k}} = \frac{4}{a}\mathbf{S_{0,k}^{-1}}; \qquad (2) \\ &\mathbf{ä}_k = \left(\mathbf{I} - \mathbf{S_{1,k}}\mathbf{S_{0,k}^{-1}}\right)^{-1}; \quad \mathbf{ó}_{eff,k} = \mathbf{ó}_k - \mathbf{F}_k; \\ &\mathbf{F}_k = (\mathbf{í_f ó_f})\mathbf{ó}_k \end{aligned}$$

Terms introduced here are easy to interpret. $\mathbf{D_k}$ is a generalized matrix of diffusion coefficients, which is full unlike the traditional diagonal one. The matrix $\mathbf{\Sigma_{af}}$ describes absorption and fission processes (including inter-group transitions) in cell. Matrix $\mathbf{\delta}$ may be called the main coarse-mesh correction. Actually in case of a single group this term is:

$$\mathbf{\delta = 1/(1-[a^2(\Sigma_a - \nu_f\Sigma_f)k_\Phi/(8Dk_j)])}$$

where $\mathbf{k_\Phi}$ and $\mathbf{k_j}$ are flux and current coefficients of irregularity. The formula for $\boldsymbol{\delta}$ looks like Askew's correction but has no peculiarity regarding mesh size. Finally, **F** is a natural generalization of neutron multiplication matrix. In order to specify the point let us derive the following chain of relations explicitly:

$$\mathbf{F}\vec{\Phi} = (\boldsymbol{\nu}_\mathbf{f}\boldsymbol{\Sigma}_\mathbf{f})(\mathbf{S_0} - \mathbf{S}_1)^{-1}(\mathbf{S_0} - \mathbf{S}_1)\vec{I}_S = (\boldsymbol{\nu}_\mathbf{f}\boldsymbol{\Sigma}_\mathbf{f})\vec{I}_S$$

It follows that $\sum_{g'}[\mathbf{F}]_{gg'} = \sum_{g'}[\boldsymbol{\nu\Sigma}_\mathbf{f}]_{gg'} I_{s,g'}$ is a term that describes a number of neutrons emitted in the g-group, since $I_{s,g}$- is an average current of neutrons inflowing (outflowing) to a g-group cell. Values $I_{s,g}$- are surely determined only after the problem is completely solved. However $\vec{\Phi} = (\mathbf{S_0} - \mathbf{S}_1)\vec{I}_s$ (which can be interpreted as a multi-group level of neutrons in cell) is unknown in equation (1) rather than $I_{s,g}$ itself. Actually neutron current on the side between cells i and k is determined by $\vec{j} = \boldsymbol{\Delta}_{\mathbf{ik}}(\vec{\Phi}_i - \vec{\Phi}_k)$, i.e. proportional to the level difference between cells i and k.

Let us conclude this subsection with pointing out some improvements in calculation of the series obtained due to SHM.

(i) Introduction of the main coarse-mesh correction $\boldsymbol{\delta}$;

(ii) Partial accounting of cell environment. Neutron spectrum in cell is represented through the sum of overlapping group spectrums with amplitudes $I_{s,g}$, i.e. it depends on environment. This environment is considered partly, as the homogenization procedure is applied to calculations of multi-group 4 (8, 15) cross-sections.

(iii) The use of non-diagonal matrixes of diffusion coefficients. Non-diagonal elements depend on the mesh size.

Higher harmonics were not taken into consideration at this stage since higher harmonics should not give significant improvement in precision under such small-mesh calculations. Non-diffusion corrections for cell boundaries are also absent. They will be accounted for in the next computational series and we are going to discuss their significance when analyzing final results.

Two additional notes should also be made here. First, effective cross-sections in the SHM, strictly speaking, depend on K_{eff}. In order to take this dependence into consideration in preceding calculations we introduced "super-outer iterations" that eventually made the $1/K_{eff}$ multiplier in the last term of equation (1) equal to one. Effective multiplication factor is determined by $\frac{1}{K_{eff}} = \prod_i \frac{1}{K_{eff}}_i$, where i is a number of super-outer iterations. The most difficult cases required not more than 3 such iterations. In this calculations no such iterations were needed at all. A single test calculation evidenced this result and thus we did not carry it out in subsequent computations. Such iterations are indeed worthless here due to K_∞ of cells equal to 1.05 unlike 1.25-1.30 in RBMK and VVER cells. At the same time above mentioned effect for effective cross-sections is proportional to $(K_\infty-1)/K_\infty$ for fuel cells and nearly vanishes for the "non-fuel" ones.

Second, we accounted for axial leakage similarly to “traditional calculations” subsection. Some analysis shows that more accurate description of this term appears to be quite unnecessary since axial leakage is rather small being proportional to

$$\sim[(K_\infty-1)\backslash K_\infty]*[B_z^2/(B_z^2+B_x^2+B_y^2)$$

3. The third series of calculations is called "SHM-heterogenous" although homogenization procedure is not excluded totally. In these calculations we again use the same values of **D** and δ as in the previous series. Consecutive computation of real heterogenous cells is carried out for deriving the set of the main symmetric trial functions of $\mathbf{S_0}$. Transport equation for G_3 SPSM approximation is solved for cells. Actually we solve the sequence of problems with given boundary currents similar to those described in preceding subsection but $f_{s,gg'}$ now determine both boundary (local) neutron levels (SHM het1) and boundary fluxes (SHM het2):

$$3\int_{4\pi}\left(\vec{\Omega}\vec{n}\right)^2\Phi_g\left(\vec{r},\vec{\Omega}\right)d\vec{\Omega}=\Phi_{0,g}+2\Phi_{2,g}\qquad\text{SHM het1}$$

$$\int_{4\pi}\Phi_g\left(\vec{r},\vec{\Omega}\right)d\vec{\Omega}=\Phi_{0,g}\qquad\text{SHM het2}$$

Here Φ_n - are n-angle Legandre solution moments. In all other respects solution procedure for heterogeneous cells is quite the same as in previous subsection. Of course, additional remarks made at the end of that subsection also become applicable. As far as SHM improvements are concerned, it should be noted that in this case cell environment is considered more properly and non-diffusion corrections (SHM het1) are involved. Note that despite the number of problems for cells is greater here than in ordinary calculations, namely G problems (4, 8, 15) that correspond to different incoming currents instead zero boundary currents this insignificantly increases time costs. It is so as far as the calculations of the Green’s functions moments $G^{p,k}{}_{n,m}(\rho'\rightarrow\rho)$, takes the most time. However these moments are the same ones for problems with different currents.

2.3. Calculation results

Tables below illustrate our calculation results. Let us start with discussion of Table 2 that shows the main results, including:

1. The group structure has a small impact on results. As follows from the data panel difference between results for 4, 8, and 15 group computations is quite small for all series and all cores. It is of special importance for the core C. Here for 4 group value δK_{eff}=11 pcm in SHM series. This means that a 4-group approximation usual for VVER calculations of energy distributions inside assemblies, especially when SHM is applied, is quite enough for getting precise results.

2. Accounting of cell heterogeneity is essential. The SHM gives small improvement of precision for homogenous lattice (core A) but provides quite significant corrections for cores B and C. This effect distinguishes more in K_∞ values for central assemblies – a quite natural result indeed. Differences in columns of SHM-homogenous from

SHM-heterogenous are 3-4 times smaller than from traditional calculation (TC) numbers. Signs of those errors are worthy more detailed discussion.

The results of traditional calculation (TC) for the core B are under predicted comparing with those of SHM-heterogenous and (even more) SHM-homogenous.

As far as results obtained for core C are concerned, error signs are opposite traditional calculations to over predict K_{eff} (and K_∞ even more for the central assembly) comparing with SHM-heterogenous and (even more) SHM-homogenous. Significant difference between results of SHM-heterogenous and SHM-homogenous (especially for K_∞) also is worthy noting. This difference includes not only cell homogenization effect but also effect that comes from considering "non - diffusionality" on cell boundaries in SHM-heterogenous calculations (see also (Laletin, 1995)). A some notion about value one can get from the comparison of numbers SHM het1 and SHM het2 of Table 2. Existing difference in errors mentioned above regarding various cores and series can be qualitatively explained if noticing that thermal neutron flux experiences most changes inside the lattice. Let us consider the behavior of those neutrons near absorber in lattice (see Figure 3) and near a water cell (see Figure 4.).

Neutron current is assumed to be proportional to the difference between average fluxes in non-fuel assemblies and adjoined fuel ones in traditional computations. The Figures show that this assumption under predicts actual currents and makes the resulting flux underestimated in the absorber and overestimated in the water. This seems to be the main cause for overvaluation of K_{eff} in traditional series for the core C and undervaluation for the core B. One more remark should be made regarding the sign of an error in traditional calculation for the core C. At first sight this result somehow contradicts the result obtained by DIF3-NODAL code, which undervalues the multiplication factor comparing with DIF3-VARIANT (under the same set of initial constants). However as follows from the name of the code DIF3-NODAL uses not a simplest finite-difference scheme as in traditional calculations.

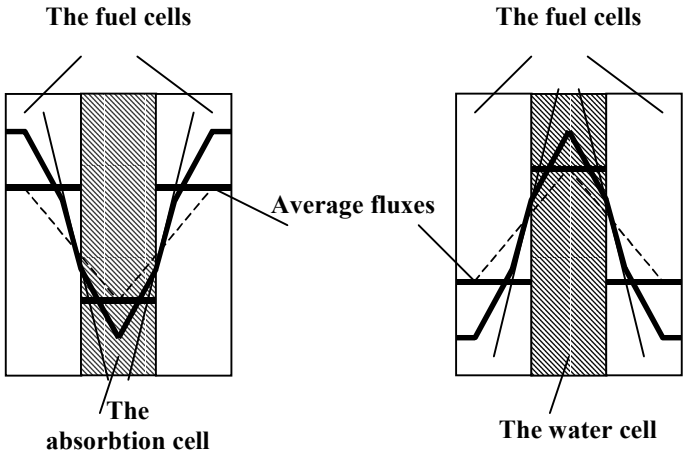

Fig.3.

Fig.4.

In this respect one should compare:

K_{eff}(DIF3-NODAL)-K_{eff}(DIF3-VARIANT)=-340pcm

with K_{eff}(SHM-gom.)- K_{eff}(SHM-get.)=-225pcm

Insignificant difference of these values seems to be acceptable. The same remark but a bit less justified can be made for result obtained by GEMESH code. Although diffusion approximation is applied there, every cell is arranged in 4 (2x2) subzones.

Table 2. Multiplication factors and errors in pcm.

Core	Groups	TC	SHM-hom.	SHM het1	SHM het2
A	4*	-14	-13	-27	-5
	8*	+7	+10	-7	0
	15**	1.00220 (-47)	1.00227 (-41)	1.00267	1.00350 (+83)
	15a*	+25	+25	+24	
	K_∞ δK_∞**	_____ _	_____	1.06029	
B	4*	+97	-29	-21	-5
	8*	+1	-9	+10	+5
	15**	0.99829 (-404)	1.00313 (+80)	1.00233	1.00264 (+31)
	15a*	+91	+67	+88	
	K_∞ δK_∞**	1.045545 (-530)	1.052189 (+135)	1.050841	
C	4*	+51	-----	-11	-27
	8*	+31	-----	+7	-10
	15**	1.00670 (+749)	0.99696 (-225)	0.99921	1.00155 (+234)
	15a*	+36	+49	+39	
	K_∞ δK_∞**	1.00413 (+1905)	0.98002 (-496)	0.98498	

*- differences from “15-group” result;

**- differences from “SHM-heterogenous” result;

The line 15a in Table 2. gives values multiplication factors and errors obtained using a library with corrected cross-sections for U-235 and U-238. It has already been mentioned that we used micro-constant library of WIMS-D4 code (proposed by the authors of the code in early 1980th) in most computations. It seems quite appropriate since many organizations, including Russian ones, have been using WIMS-D4 code with that library until recently. However yet in 1980th we had analyzed the system of constants for WIMS-D4 code and modified U-235 and U-238 cross-sections trying to come closer to the constants of neutron-physics cross-sections bank of Kurchatov Institute. Actually those constants with modified cross-sections for U-235, U-238 were the best in describing the whole experimental data set (multiplication factors and spectral indices ρ^{28}, C*, δ^{25}, δ^{28}) for the known thermal cores TRX, BAPL (Laletin,,

1983). Those constants have been used in computations that gave results presented in the line 15a of Table 2 and in column WIMS-D4C (correction of cross-sections of U-235 and U-238) of Table 3. The latter Table also shows errors comparing with the work (Mosteller , 1998) (MCNP code, ENDF/B-V1.3 cross-section). Errors for values correspondent to initial WIMS's constants are also presented there.

Table 3. Differences of spectral indices for various constant libraries comparing with MCNP (Mosteller , 1998) results (ENDF/B-V1.3)

Core	Parameter	Value (Error, %)	
		WIMS-D4	WIMS-D4C
A	K_∞	1.06036 (416 pcm)	1.06010 (410 pcm)
	δ_{25}	0.130 (-0.5)	0.130 (0.03)
	δ_{28}	0.0640 (-1.3)	0.0624 (-3.9)
	ρ_{25}	0.350 (-3.0)	0.354 (-2.1)
	ρ_{28}	2.186 (-4.0)	2.290 (-0.1)
	CR	0.457 (-2.8)	0.469 (-0.3)
B	K_∞	1.05084 (424 pcm)	1.05176 (457 pcm)
	δ_{25}	0.116 (0.8)	0.116 (0.5)
	δ_{28}	0.0589 (-2.0)	0.0575 (-4.4)
	ρ_{25}	0.312 (-2.6)	0.317 (-1.4)
	ρ_{28}	1.948 (-4.7)	2.044 (-0.03)
	CR	0.428 (-3.0)	0.439 (-0.4)
C	K_∞	0.98498 (78 pcm)	0.98436 (16 pcm)
	δ_{25}	0.130 (1.3)	0.129 (0.8)
	δ_{28}	0.651 (-1.1)	0.0633 (-3.7)
	ρ_{25}	0.350 (-2.4)	0.354 (-1.3)
	ρ_{28}	2.188 (-4.3)	2.291 (0.2)
	CR	0.456 (-2.9)	0.468 (-0.3)
	PAF	0.140 (1.0)	0.139 (0.4)

The line 15a of Table 2. shows that multiplication factors are changed very little when the new constant set is used. At the same time values from SHM-heterogenous column are much closer to experimental ones (1,0007±2*0,0006) comparing with values based on ENDF/B-V1.3 cross-sections (Parish, 1998). Perhaps this illustrates desirability of increasing ν_f for U-235 in the thermal neutron zone in the system of ENDF/B-V1.3 (the value $-\nu_f$ in the MCU-RFFI (Glushkov, 1995) code virtually coincides with corresponding value in this system). As it has already been mentioned, this recommendation agrees with results of TRX and BAPL cores calculations.

As far as spectral indices of Table 3. are concerned, perfect matching of WIMS-D4C and MCNP (Mosteller, 1998) indices worth noting. Errors for WIMS-D4 are large enough (and quite expectably indeed) especially for ρ^{28} and C^*_R.

In Table 4 some mean values for pin-by-pin power distributions are presented. These distributions are not so informative ones in our opinion but the analogues distributions in other papers also. It flows from a comparison of experimental and calculation errors. The main calculation errors are in absorber rods, as one can see from values PAF.

Table 4. The ratio of maximal power-distribution to average and its error; 15-group calculation

Core configuration		B	C
W_{peak}	TC	1.093	1.131
	SHM-hom	1.101	1.184
	SHM het1	1.098	1.173
	EXP	1.108	1.158
δW_{peak}, %	TC	-1.3	-2.3
	SHM-hom	-0.6	2.2
	SHM het1	-0.9	1.2

The location of the peak pin, predicted by the SHM, coincide with the location of the experimental peak pin.

ACKNOWLEDGMENTS

Authors are grateful to Dr. T.Taiwo, which was a initiator of carrying out of this work and International Safety Center for support of this one. We would like to thank the Russian Fund Fundamental Research for partial support of our paper (Grants #99-01-00348, #01-01-00623)

REFERENCES

[Diamond, 1996] D.J. Diamond, Letter dated July 19, 1996 on "PWR Lattice Benchmark Problem" prepared by Ad Hoc Committee on Reactor Physics Benchmarks

[Glushkov, 1995]A.E.Glushkov, E.A.Gomin, M.I.Gurevich, L.V.Maiorov, 1995 Annotation of MCU-RFFI-code», VANT, v. 3, p. 48

[Laletin, 1983] N.I.Laletin,, V.A.Lulka, 1983 The analisis of comparison of calculational and experimental characteristics of assemblyes TRX, MIT», In book "Experimental reactor physics", Moskow Atominform, p.59, See also I.A.Zhokina, A.I.Popykin, A.I.Tatourov, "Correction and verification of U-235 and U-238 nuclides for library of WIMS code", internal report RRC KI

[Laletin, 1990] N.I.LALETIN,N.V.SULTANOV,V.F.BOYARINOV."Surface Harmonic and Surface Pseudo-Sources Methods."-Proceedings of International Conference on the Physics of Reactors,v.2,pp.XII-39-XII-48,April 23-27, Marsille, France, 1990.

[Laletin, 1995] N.I.Laletin, N.V.Sultanov, A.Yu.Kurchenkov, 1995 Nondiffusional Correction by. Fine Mesh Calculations of VVER Lattices, Proc. of Inter. Conf. on Mathematics, and Computations, Reactor Physics, and Environmental Analyses, April 30-May 4, Portland, Oregon, USA, p. 813.

[Laletin, 1998] N.I.Laletin Analysis of the Surface Pseudosources Method (Gn - Approximations) and Comparison with Other Numerical Methods for the Neutron Transport Equation. TTSP,V 27, N. 5-7,p.639,1998

[Laletin, 1999] N.I.Laletin, N.V.Sultanov, A.A.Kovalishin, 1999 Surface Pseudosources and Surface. Harmonic Methods, Report of International Nuclear Safety Center of Minatom. of Russia, Joint project #2, Phase 3, Task 17, Moscow, Russia,

[Mohanakristan, 1998] P.Mohanakristan, S.M. Lee, 1998 PWR Lattice Benchmark Solutions", Ibid. p.1268

[Mosteller, 1998] Russell D. Mosteller , 1998 ENDF/B-V and ENDFB/-VI results for UO_2 lattice benchmark problems using MCNP, Proc. Int. Conf. on Nuclear Science and Technology, 5-9 Oct. 1998, Long Island, New-York, p.1282

[Paris, 1998] T.A. Parish, D.J. Diamond, R. D. Mosteller, J.C. Gehin, 1998 Summary of Resilts for the Uranium Benchmark Problem of the ANS AdHoc Committee on Reactor Physics Benchmarks, Ibid., p.

[Taiwo, 1998] T.A. Taiwo, R.N. Blomquist, G. Palmiotti, J.R. Deen, 1998 Analysis of ANS LWR Physics Benchmark Problems, Proc. Int. Conf. on Nuclear Science and Technology, 5-9 Oct. 1998, Long Island, New-York, p.1261.